Bending moments in lower extremity bones for two standing postures

M. Munih, A. Kralj and T. Bajd

Faculty of Electrical and Computer Engineering, University of Ljubljana, Slovenia

Received May 1991, accepted October 1991

ABSTRACT

The goal of this paper is to study how external gravitational forces stress the lower extremity bones and to ascertain and study how muscle activation compensates for the external load. For these purposes relatively accurate anatomical and biomechanical modelling is necessary. For a comparison of the calculated results to the naturally occurring muscular activity, seven-channel surface EMG activity was recorded. For simplicity a two-dimensional model was developed for the sagittal plane including 19 lower extremity muscles relevant to human standing and walking. In the calculation procedure of muscle forces an optimization procedure is also included. The results give rise to the expected assumption that muscle action is covered by two main requirements: first, to stabilize the joint actively (moment equilibrium) and, second, to compensate efficiently for bending moments produced by gravitational and external forces.

Keywords: Bending moment, musculo-skeletal system, biomechanical modelling

INTRODUCTION

Only a few researchers in the past have studied the close collaboration of bone and skeletal muscle. Galileo Galilei, in 1638, according to Baron[1], was the first and already at that time related the bone shape to the corresponding muscle function. More profound studies on bone stress were published later by Koch[2]. Very detailed and far-reaching functional interpretations of bone, bone loading and muscle action were first clearly expressed and explained by Pauwels[3], whose theoretical studies have led to the hypothesis that the biomechanically important function of the muscle is the minimizing of the dangerous bending moment loading of the long bones. Furthermore, Pauwels concluded that the bending moment profiles are invariant and independent of the posture selected or movement performed. This basic idea of long bone unloading by means of active muscle forces is the fundamental principle of bone-muscle function; it is illustrated in *Figure 1*. In *Figure 1a* a gravitational force is loading the bone with the bending moment M_G, while in *Figure 1b* the muscle moment M_M is acting in the opposite direction. If moment levers are fixed and equal, the resulting bending moment M_S theoretically equals zero, while the compression stressing is doubled (*Figure 1c*). As in the case described, it is evident that muscle activity is the key principle that results in a significant saving of bone material. The same law applies also to more complicated bone shapes and to synergistic muscle activation due to bone shape and muscle attachment geometry, which is consequently necessary for achieving efficient bone unloading and muscle function.

This paper discusses the *in vivo* testing of the above principles through biomechanical modelling and the calculation of bending moments for the femur and the tibia in the sagittal plane, including 19 lower extremity muscles. For model composition, detailed and accurate anatomical measurements on specimen and kinesio-logical measurements on healthy subjects were made. Numerical data were assessed for five male subjects in two static standing postures: normal upright standing and standing while leaning forward.

METHODS

For the bending moment calculation of the lower extremity long bones a specific model was developed, since the published and existing musculo-

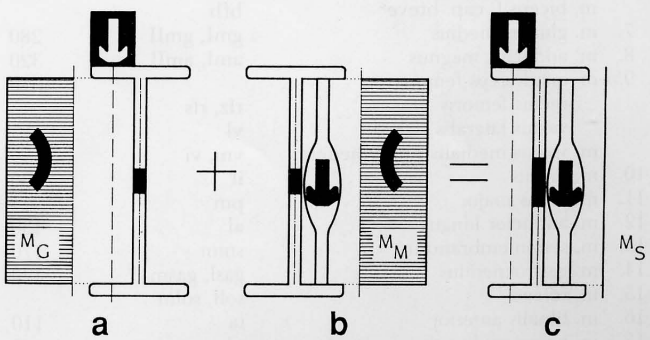

Figure 1 Bending moment caused by an external load (a) is effectively compensated (c) by muscle force (b). Moment lever is constant and equal in all cases. Gravitational force equals the muscle force. The bending moment compensation principle was clearly explained for the first time by Pauwels[3]

Correspondence and reprint requests to: Marko Munih, MSc, Faculty of Electrical and Computer Engineering, Tržaška 25, 61000 Ljubljana, Slovenia

0141–5425/92/04293–10

skeletal models cannot be directly implemented because of missing data or scaling problems. Most of the published mathematical models of the lower extremities deal with the dynamic properties relevant to a description of gait[4,5,6]. The models usually include gravitational and inertial forces or moments together with centrifugal and Coriolis contributions and ligament moments. In some of these models the muscle's action is also taken into account[5,6]. In most cases the muscle is described by a model consisting of an active contractile element in series with elastic and viscous damping, originally proposed by Hill[7]. On the other hand several authors calculate muscle forces through different optimization procedures[8,9,10,11,12,13]. They use different types of linear or nonlinear optimization functions. Our model, which incorporates knowledge gained from published models, includes a linear muscle coordination optimization technique and the bending moment calculation of long bones. The model and procedures carried out will be described in four steps: the anatomical and the kinesiological measurements of the required data for modelling, the muscle force optimization and the bending moment calculation.

Anatomical measurements

For calculating the bending moments, a musculoskeletal model accurate in details to the anatomy of the subject's lower extremity is necessary and was therefore developed. The muscle force and moment calculations performed include the determination of the following elements:

- exact muscle attachments including shapes, positions and orientations;

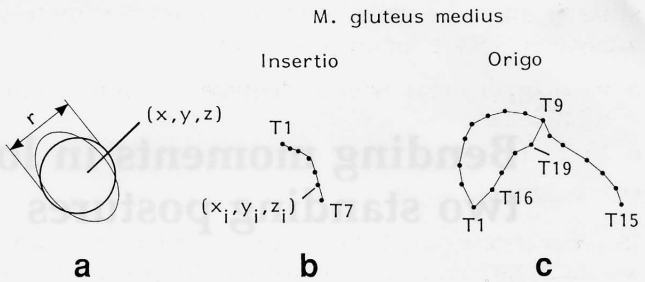

Figure 2 Muscle attachments as measured and represented by the computer. Very small attachment areas were included as the central point (x, y, z) with diameter r as in case (a). Long and narrow attachments consist of several points measured a long the line (b). Larger areas as in (c) were bordered with several points.

- exact bone dimensions and shapes;
- points of the resultant muscle force activity;
- directions of the muscle force vectors.

In the existing literature there are numerous models published, but in most cases they lack accurate numerical anthropometric data for the main muscle attachments along the bones of the lower extremity. Therefore we decided to measure all the data required. For this purpose a specimen of the right lower limb of a 26-year old male subject was selected and placed into a reference position with the help of a specially designed measuring frame. First the muscles were carefully dissected, one by one, along natural layers, from the specimen. After each muscle was dissected, the attachment circumferences were marked with pins inserted up to 10 mm apart. The coordinates x, y, z of the pins were precisely measured by a caliper with respect to the measuring frame with the accuracy better than ± 0.25 cm and manually entered into the computer. The measured points assessed were, in a CAD program, connected by

Table 1 Volume, tendon length, cross-section and estimated maximal force of dissected lower limb muscles

No.	Muscle	Abbreviations	Volume [ml]	Tendon [mm]	Cross-section [mm^2]	Fmax [N] 30 N cm^{-2}	Fmax [N] 50 N cm^{-2}
1.	m. sartorius	sar	125	75	240	72	120
2.	m. gracilis	ga	80	100	270	81	135
3.	m. semitendinosus	smt	170	150	660	198	330
4.	m. gluteus max.	gma	620	—	4944	1483	2472
5.	m. tensor fasciae latae	tfl	75	385	330	99	165
6.	m. biceps f. cap. longum	bfl	220	36	630	189	315
	m. biceps f. cap. breve	bfb		36	300	90	150
7.	m. gluteus medius	gmI, gmII	280	—	2170	651	1085
8.	m. adductor magnus	amI, amII	320	80	1540	462	770
9.	m. quadriceps femoris		1650	—	4340	1302	2170
	rectus femoris	rfz, rfs		—	720	216	360
	vastus lateralis	vl		—	930	279	465
	m. vastus medialis + intermedius	vm, vi		—	1750	525	875
10.	m. iliacus	il	200	—	770	231	385
11.	m. psoas major	pm	*	—	930	279	465
12.	m. adductor longus	al	130	15	760	228	380
13.	m. semimembranosus	smm	170	102	750	225	375
14.	m. gastrocnemius	gasl, gasm	420	145	1190	357	595
15.	m. soleus	soll, solm		50	1470	441	735
16.	m. tibialis anterior	ta	110	104	540	162	270
17.	m. peroneus longus	pl	60	212	220	66	110
18.	m. peroneus brevis	pb	40	60	120	36	60
19.	m. flexor digitorum longus	dl	70	†	240	72	120

*Used only lower section of muscle
†Fanlike insertion

straight lines. In general three shapes for muscle attachments were found (see *Figure 2*):

- very small areas with a diameter of only a few millimetres;
- large attachment areas;
- attachment curves.

In the first case only the centre of the attachment was assessed together with the corresponding diameter. In the second case several coordinates were measured along the circumference of the attachment area. In a similar way the coordinates were assessed also along the attachment curves. Most of the muscles had the third type of attachment while very small attachment areas were rarely presented. Several muscle attachments, such as those from m. gm, m. am, m. rf, m. gas and m. sol (for classification of abbreviations see *Table 1*), consisted of combined attachments or had two muscle insertions or origins. These were the reasons for dividing some muscles, considering them as consisting of two muscles and labelling them as gmI, gmII, amI, rfz, rfs, gasl, gasm, solm, and soll. Muscle gm consisted of a large attachment area and a thick attachment curve as shown in *Figure 2*, while m. am had two different insertions. Muscle rf had two origins, and the muscles m. sol and m. gas were divided into lateral and media parts because of the corresponding lateral and medial insertions. For each muscle separated from the specimen the following characteristic parameters were determined (*Table 1*): the anatomical maximal cross-section area, the muscle volume and the muscle tendon.

The next task was to determine numerical data representing the shapes of the lower limb bones, the femur and the tibia. To assure the same accuracy of measurements and for the sake of simplicity, the necessary numerical data were gathered in the same way and by the same instrumentation as the data describing the muscle attachments. The model was built in the sagittal plane, so that the anterior part of the femur was represented by 20 points, the posterior part by 28 points. Similarly, the shape of the tibia was modelled with 20 points in the posterior part and 17 points in the anterior part. The bone shape in the joint area was excluded because it was not possible to measure the bone shape in the joint area with the same accuracy as for the straight part of the bone. Determination of the femoral and tibial bone shapes around the hip, knee and ankle joints was improved by increasing the number of points by reading the joint bone shape from a close-up X-ray photograph. This was utilized since the X-ray picture taken for the whole bone could not yield sufficiently accurate data because of nonlinearities in the photographing system. Anterior and posterior points were later interpolated (natural cubic spline) at the same height z. In this way points along the bone's central line (*Figure 3*) were calculated. These points were very important because all the bending moments were calculated through the levers determined according to this central line.

The fibula was not included in the present model. The calculation of the distribution of the muscle forces between the tibia and fibula would considerably complicate the already complex mathematical

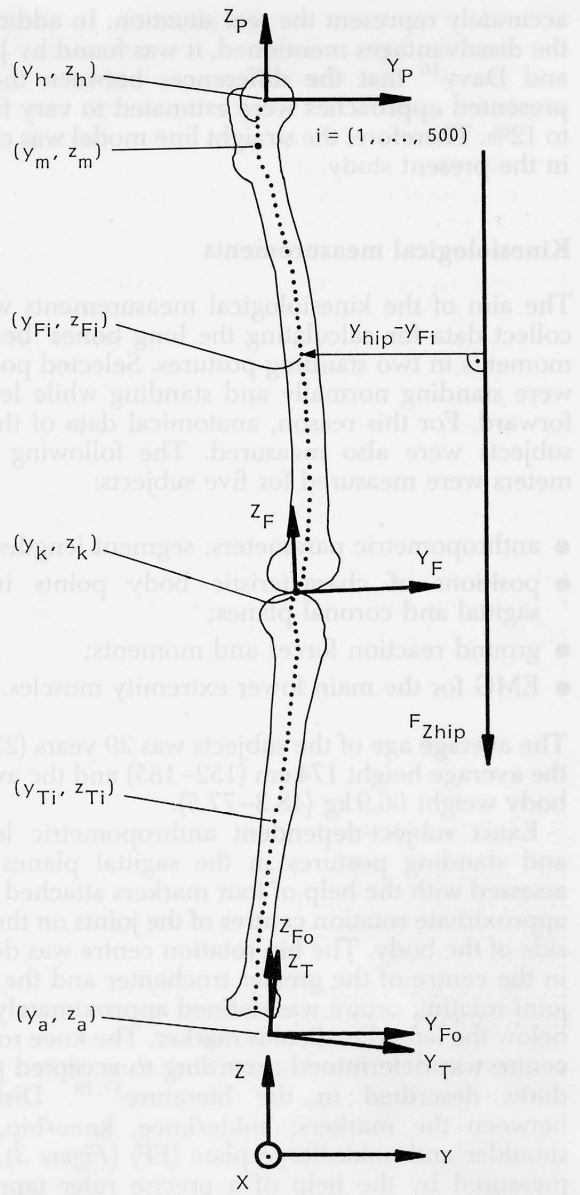

Figure 3 Femur and tibia bone shapes with bones' central line points, markers for hip (y_m, z_m), knee (y_k, z_k) and ankle (y_a, z_a), and coordinate systems placed in ankle, knee and hip rotation centres. F_{Zhip} represents the vertical component of the ground reaction force; (y_h, z_h) = head of femur; (y_{Fi}, z_{Fi}) = ith point on femur central line; (y_{Ti}, z_{Ti}) = ith point on tibia central line

model. The skeletal muscles having attachments on the fibula were treated as belonging to the tibial bone.

From the data gathered, it is possible to determine the directions of the muscle force activity. In general two approaches are possible: (a) the straight line model; and (b) the centroid model. In the first case a straight line passes between two muscle attachments[14,15]. The centroid line model requires that the positions of the transverse cross-sectional centroids are established for each muscle. The muscle force is represented by a tangent to the centroid line at the point of interest. The complexity of the lower limb model, including 19 muscles, would increase considerably by taking into account the centroid model. Furthermore, the centroid line model obtained from a cadaver may not

accurately represent the real situation. In addition to the disadvantages mentioned, it was found by Jensen and Davy[16] that the differences between the two presented approaches were estimated to vary from 1 to 12%. Therefore, the straight line model was chosen in the present study.

Kinesiological measurements

The aim of the kinesiological measurements was to collect data for calculating the long bones' bending moments in two standing postures. Selected postures were standing normally and standing while leaning forward. For this reason, anatomical data of the test subjects were also measured. The following parameters were measured for five subjects:

- anthropometric parameters: segment lengths;
- positions of characteristic body points in the sagittal and coronal planes;
- ground reaction forces and moments;
- EMG for the main lower extremity muscles.

The average age of the subjects was 29 years (23–43), the average height 174 cm (152–185) and the average body weight 66.9 kg (48.3–77.5).

Exact subject-dependent anthropometric lengths and standing postures in the sagittal planes were assessed with the help of four markers attached to the approximate rotation centres of the joints on the right side of the body. The hip rotation centre was defined in the centre of the greater trochanter and the ankle joint rotating centre was defined approximately 1 cm below the lateral malleolus marker. The knee rotating centre was determined according to accepted procedures described in the literature[17,18]. Distances between the markers: ankle/knee, knee/hip, hip/shoulder and ankle/force plate (FP) (*Figure 3*), were measured by the help of a precise ruler tape with a ± 0.5 mm accuracy. Marker coordinates were assessed through black and white photography in the sagittal plane. The cameras were aligned according to plumb lines for vertical accuracy. The photographically obtained coordinates were entered into the computer with the aid of magnifier film projection (Dorst Laborabor 1000) on to a graphic tablet (Cherry mkIII). Six points were recorded in each frame. Along with the four points mentioned, two additional points of the plumb line, representing the direction of gravity, were recorded. From the data obtained, ankle, knee and hip angles during standing were calculated. All data were translated to a global coordinate system and the moments were calculated in the global coordinate system. The +Z axis of the global coordinate system was perpendicular to the force plate. +Y and the measured person were directed forward, with $y = 0$ at the ankle marker. Therefore, the anatomical data previously assessed in the cadaver could be scaled and rotated according to the anthropometric data belonging to the particular standing posture of each subject. Distances between anatomical markers were used for linear scaling of the cadavers' numerical data, i.e. the femoral and tibial centre lines and the muscle origins and insertions.

The action point and magnitude of the ground reaction force (F_z value) and the point of its action at shank and thigh height are needed in our model in order to calculate the bending moments along the long bones of the lower extremities. F_z and M_x are the ground reaction (z) force and (x) moment. The computer model incorporates different segment density values. Each limb segment has a different combination of bone, muscle, fat and other tissue components. More distal segments have a higher density. This consideration was included in the F_z force calculation. In accordance with Winter[19], foot (d_F), shank (d_S) and thigh (d_T) densities as functions of the total body height and weight were determined. An AMTI (Advanced Mechanical Technology OR6-5-1) force plate with strain gauge transducers was used for ground reaction measurements. The subject was asked to place the right leg on the FP and the left leg on a wooden support the same size as the FP. The angle between the left and right foot was always 30°. Both feet were placed with heels together in such a way that the anterior/posterior y_a coordinate was aligned with the centre of the FP. Before the measurement all the markers were placed and the anthropometric data measured. The subject was asked to remain in the same posture for one minute. In that time the force plate parameters were collected by the computer and photographs were taken after 20 s and 40 s. According to our observations, 20 s was enough time for posture stabilization. The second photograph was taken after 40 s for posture stability checking. As mentioned earlier, the selected postures were standing while (i) leaning forward and (ii) standing normally.

EMG activity assessment

The EMG activity during each measurement of the standing procedure was recorded for seven muscles: m. gastrocnemius, m. tibialis anterior, m. vastus medialis, m. rectus femoris, m. semimembranosus, m. biceps femoris and m. latissimus dorsi. We used seven channels of the laboratory eight-channel integrating EMG system with an adjustable gain (1000–20 000) and the time constant of the integrator was set to 20 ms for this purpose. Surface electrodes were E221 (In Vivo Metric).

Gravitational bending moment calculation

In any upright static standing posture gravitational forces tend to lower and collapse our body segments. The action of muscles counterbalances the gravitational forces and moments, and thus maintains stability and additionally serves for movement control but also produces stress in bones. We are interested to determine the bending moments along the bones: the femur and the tibia. It is evident that the resultant bending moment acting on the bone is a sum of:

- the bending moment caused by gravitational force;
- the bending moments caused by muscle forces.

The bending moments are calculated along the bone's centre line (*Figure 3*). The femur's or tibia's centre line consists of 500 equidistant points z_{Fi} measured in the vertical direction (*Figure 3* – index F is used for the femur and T for tibia, $i = 1, 2, \ldots, 500$). The point z_{F1} is the highest measured from the supporting surface and z_{F500} the lowest. The distance between two neighbouring points is less than 1 mm. The F_Z force, representing half of the body weight, was determined as an average over 1 s of the vertical force on the force plate. The gravitational force $F_{Z\text{hip}}$ in the hip results from the trunk, arms and head weight, without the thigh m_T, shank m_S and foot m_F contributions. $F_{Z\text{knee}}$ acting in the knee is larger because of the mass value m_T. From the force plate, data average values of the ground reaction force application $\bar{y}_{Fz}$ can be determined. With the help of Winter's[19] data, the mass centres for the foot y_F, shank y_S and thigh y_T can be calculated in reference coordinates. This is necessary in order to determine the coordinate y_{hip} of the force $F_{Z\text{hip}}$ acting at the hip level. Similarly, y_{knee} can be found for the force $F_{Z\text{knee}}$ acting at the knee level. When all the necessary data and parameters are calculated, the gravitational moment M_{Gi} is defined as (*Figure 3*):

$$M_{Gi} = (y_{\text{hip}} - y_{Fi})\, F_{Z\text{hip}} + M_{Vi}, \quad i = 1, 2, \ldots, 500 \qquad (1)$$

M_{Gi} gravitational moment at the ith point,
M_{Vi} partial gravitational moment (see following text),
$F_{Z\text{hip}}$, $F_{Z\text{knee}}$ gravitational force in hip and knee joints,
y_{hip}, y_{knee} $F_{Z\text{hip}}$ and $F_{Z\text{knee}}$ action coordinates,
(y_{Fi}, z_{Fi}) ith point on the femur's central line,

for the points (y_{Fi}, z_{Fi}) on the femur's central line. The first part of the equation (1) belongs to the moment caused by the trunk, arms and head weight acting at the $(y_{\text{hip}} - y_{Fi})$ moment lever. The second part of the equation (M_{Vi}) needs a more detailed explanation. The thigh and shank can be modelled as inverted truncated cones. In the case where the moment M_{Gi} is calculated in the middle of the thigh, then only the part of the cone with its mass density d_T, volume V_i and mass centre y_{ti} above the calculated point should be included. The density d_T is determined from Winter's[19] data and V_i is calculated from the segmental mass. The moment M_{Vi} is determined as:

$$M_{Vi} = (y_{ti} - y_{Fi})\, d_T\, V_i\, g \qquad (2)$$

d_F, d_S, d_T foot, shank and thigh densities,
V_i partial volume of the truncated cone,

In the same way the moment M_{Gi} along the tibia's central line can be expressed using the shank density d_S and volume values.

The dilemma of muscle activity optimization and muscle bending moment calculation

Before determining the muscle bending moments, the muscle forces F_{Mj} (M stands for muscle and j indicates the muscle number) should first be calculated. Because there are fewer equations available than there are known muscle forces the problem can be solved by incorporating optimization procedures. There are numerous possibilities for performing the optimization. Optimization methods based on different linear or nonlinear optimization functions have been utilized by different authors[4,6,9,10,20]. Our goal was not to develop complicated and sophisticated muscle models, optimization functions and criteria, rather we were looking for a gross confirmation of Pauwel's theory. Therefore, we selected simple linear optimization techniques for our calculation of the muscle forces.

For moment equilibrium calculation in extreme joint positions (small and large angles), passive moments caused by joint ligaments are of the utmost importance[21,22]. These passive moments differ from person to person, but can be roughly approximated by mathematical equations. The hip passive moment M_{L3} and knee passive moment M_{L2} were modelled after Hatze[5]. The ankle passive moment $M_{L1} = 0$ was assumed in the ankle joint. From the known muscle moment lever r_{1j} of the joint, passive moment M_{L1} and gravitational moments M_{G1} (labels are for the ankle joint), the equilibrium equations for each joint can be written in the following form:

$$\sum_{j=1}^{28} r_{1j} F_{Mj} + M_{L1} + M_{G1} = 0 \qquad (3)$$

$$\sum_{j=1}^{28} r_{2j} F_{Mj} + M_{L2} + M_{G2} = 0 \qquad (4)$$

$$\sum_{j=1}^{28} r_{3j} F_{Mj} + M_{L3} + M_{G3} = 0 \qquad (5)$$

M_{G1}, M_{G2}, M_{G3} ankle, knee and hip joint gravitational moments,
M_{L1}, M_{L2}, M_{L3} ankle, knee and hip joint passive moments,
F_{Mj} jth muscle force,
r_{1j}, r_{2j}, r_{3j} ankle, knee and hip muscle moment levers.

In addition to these equations 28 inequalities (describing 19 muscles, some of them divided into two parts) for limiting and determining the possible range of active muscle force are defined:

$$0 \leq F_{Mj} \leq F_{Mj\max}, \quad j = 1, 2, \ldots, 28 \qquad (6)$$

where $F_{Mj\max}$ is maximal muscle force:

$$F_{Mj\max} = A_j \sigma \qquad (7)$$

$F_{Mj\max}$ maximal jth muscle force,
A_j jth anatomical muscle cross-section,
σ muscle strain,

calculated from the measured anatomical muscle cross-section A_j given in *Table 1*. Values of 30–150 N cm^{-2} can be found in the literature[4,9,10,23,24] for σ. In our work we were mostly considering $\sigma =$ 30 N cm^{-2} as the most frequently used value.

With the three equations (3), (4) and (5) and 28 inequalities (6), 28 unknown forces F_{Mj} cannot be

determined by a straightforward unique solution. Therefore, in order to select the 'best suitable solution' it is necessary to introduce some optimization procedure. For our purposes a simple linear optimization function (8) was selected:

$$f = \sum_{j=1}^{28} (F_{Mj}) \rightarrow \min \tag{8}$$

The 'cheapest' muscle is selected until its $F_{Mj\max}$ is reached, then another muscle is coactivated in order to satisfy the equations (3), (4) and (5). The optimization procedure selects the 'cheapest' muscle, which means here the most energy efficient muscle. When compared with the other muscles considered, it produces the same moment with less force, because it has the largest moment lever. This approach represents a simple synergistic muscle action criterion. The system of equations was solved by linear programming methods.

For the known muscle force F_{Mj} and the known muscle force lever r_{ji}, the muscle bending moment can be determined by:

$$M_{Mji} = r_{ji} F_{Mj} \tag{9}$$

M_{Mji} jth muscle bending moment at the ith point,
r_{ji} jth muscle force lever at the ith joint.

The determination of the muscle force lever r_{ji} is shown in *Figure 4*. The muscle force F_{Mj} is considered as acting from the known and previously calculated origin towards the muscle insertion. The muscle lever represents the distance from the force to the point at which the moment is calculated. When calculating the muscle moment close to or at the origin and the insertion area of a muscle, a special case appears. F_{Mj} is smaller than total muscle force, because in that area only part of F_{Mj} is stressing the bone. Correspondingly, the attachment coordinate of F_{Mj} force is shifted.

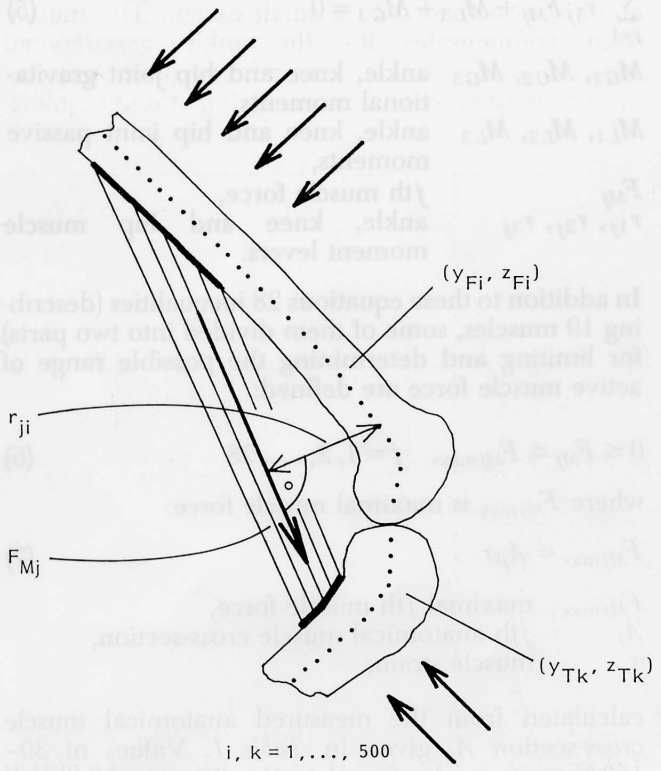

Figure 4 How muscle lever and muscle force action are determined. Muscle lever is distance from a point on the bones' central line to the force. It is perpendicular to the force F_{Mj}. Muscle force considered in the muscle moment calculation is smaller than F_{Mj} near (in) in the attachment area

RESULTS AND DISCUSSION

First we are going to present the calculated bending moments in the same order as they have been calculated. The bending moments are composed of: gravitational bending moments M_G (equations 1, 2), and muscle bending moments M_M (equation 9). The sum of both moments M_S results in the actual long bone bending moment which is stressing the bone. Bone material stress directly depends on M_S. It is known that excessive stress can provoke damage[26,27] and fracture of a bone and produce irreversible pathological changes.

The measured and calculated bending moments in two positions, normal and leaning forward, are presented for five healthy subjects. In both postures the optimization function (equation 8) was used. The muscles not presented in *Figures 5* and *6* were not selected by the optimization criteria and are, therefore, not 'active' and accordingly do not contribute to the bending moments M_M. The bending moment produced by each muscle selected from 19 muscles of the lower limb (some divided into two parts) are shown in *Figures 5* and *6*. *Figure 5* presents bending moments obtained for the postures voluntarily selected by the subjects. The ground reaction vector (GRV) represented by the vertical line passes in all cases in front of the ankle and hip joints. This is not always true for the knee joint, where in *Figure 5a* the GRV lies considerably behind the knee joint. For the ankle and hip joints the same can be concluded also for standing subjects when they were strongly leaning forward (*Figure 6*). Here, the GRV is always in front of the knee joint. For the forward-leaning standing position, depicted in *Figure 6*, $\sigma = 100\,\mathrm{N\,cm^{-2}}$ was used in equation (7). The value $\sigma = 30\,\mathrm{N\,cm^{-2}}$ used for the normal standing posture was not found high enough to solve the optimization problem as specified by equations (3), (4), (5), (6), (7), (8) for the forward-leaning standing position. In that posture, higher joint moments must be counterbalanced by muscle action than in normal standing. Therefore, according to equation (7), for developing higher F_{Mjmax} the stress σ should also be increased. The results show that in all cases the calculated muscle forces successfully counteract the passive bending moments along the long bones. Observing *Figure 5a* one part of the m. am (amII) is activated to compensate the hip gravitational bending moment. This muscle has the largest hip level in the posture measured. The muscle vl is activated in the knee as the most effective and hence energy 'cheapest' m. quadriceps muscle. The small contribution of m. vm was added to the optimization process. It is enough to activate only one part of m. sol (solm) to counterbalance the ankle gravitational

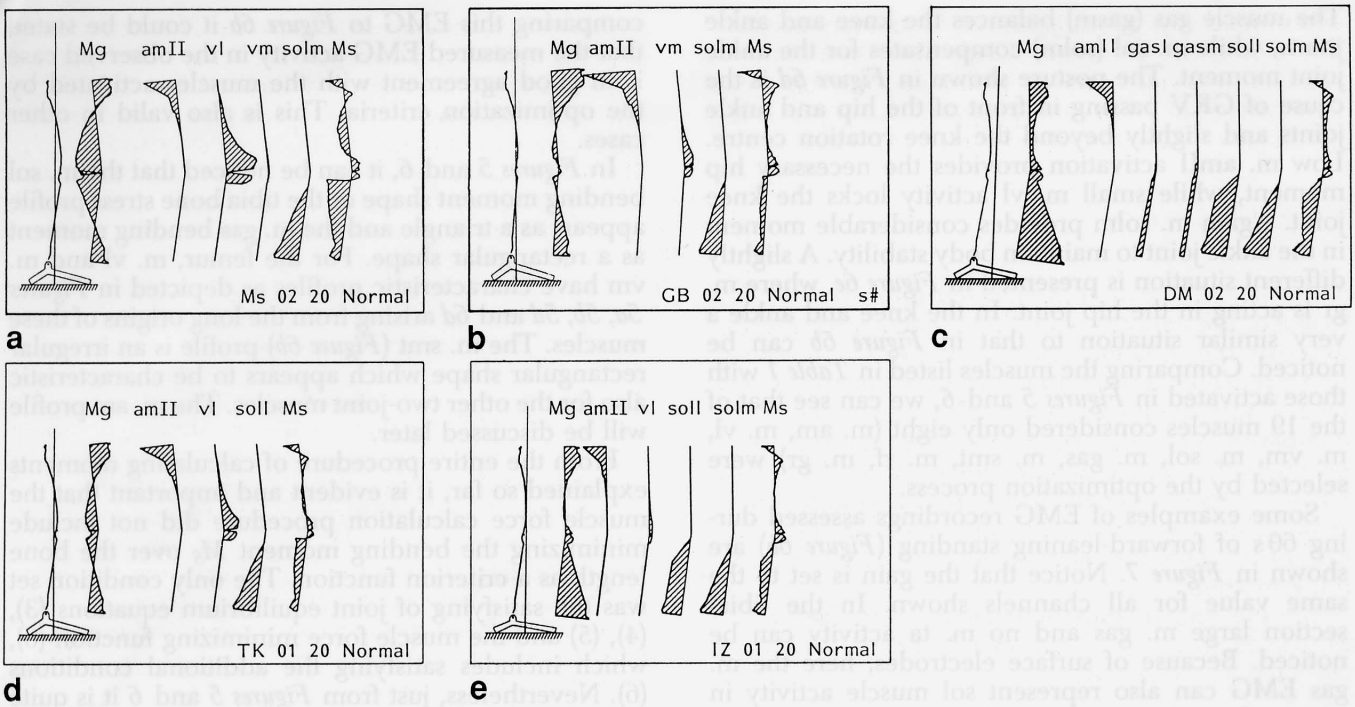

Figure 5 Gravitational, muscle and resultant bending moments for five subjects, measured and calculated during *normal standing posture*. Muscle labels are described in *Table 1*

moment. In *Figure 5b* the same situation occurs in the hip and ankle joint. A slightly different muscle activation appears in the knee joint, where m. vl alone counterbalances the small gravitational moment. An interesting situation occurs in *Figure 5c*, where m. gas (gasl and gasm) is active instead of m. quadriceps. This happens because the GRV is acting in front of the knee in that posture. A similar situation to that presented in *Figure 5a* appears also in *Figure 5d*. The activation of m. vl is sufficient to compensate for the knee gravitational bending moment. Observing *Figure 5e*, again m. am (amII) is active, accompanied slightly by the activity of m. vl and, as in case *5c*, by the whole m. sol. In *Figure 6a* the GRV passes through the knee joint. Only m. amII and m. solm are sufficient to assure the necessary muscle moment. The same is valid for the knee joint in *Figure 6c*. Because the GRV here passes slightly behind the hip, m. rf (rfz and rfs) is activated to a small extent. The muscle solm compensates for the ankle gravitational moment. In *Figure 6b* the two-joint m. smt is active as the 'cheapest' muscle crossing the hip and knee joints.

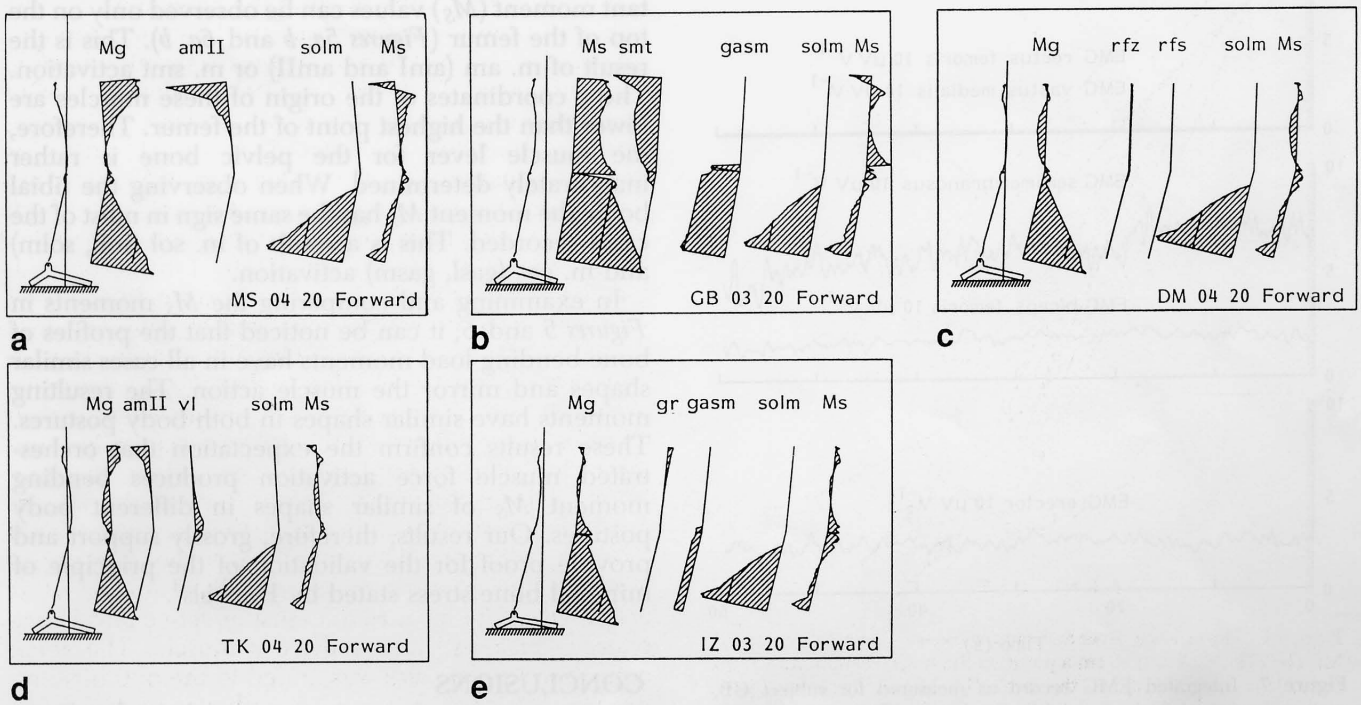

Figure 6 Gravitational, muscle and resultant bending moments for five subjects, measured and calculated when *leaning strongly forward*

The muscle gas (gasm) balances the knee and ankle joints, while m. sol (solm) compensates for the ankle joint moment. The posture shown in *Figure 6d* is the cause of GRV passing in front of the hip and ankle joints and slightly beyond the knee rotation centre. Low m. amII activation provides the necessary hip moment, while small m. vl activity locks the knee joint. Again m. solm provides considerable moment in the ankle joint to maintain body stability. A slightly different situation is presented in *Figure 6e*, where m. gr is acting in the hip joint. In the knee and ankle a very similar situation to that in *Figure 6b* can be noticed. Comparing the muscles listed in *Table 1* with those activated in *Figures 5* and *6*, we can see that of the 19 muscles considered only eight (m. am, m. vl, m. vm, m. sol, m. gas, m. smt, m. rf, m. gr) were selected by the optimization process.

Some examples of EMG recordings assessed during 60 s of forward-leaning standing (*Figure 6b*) are shown in *Figure 7*. Notice that the gain is set to the same value for all channels shown. In the tibial section large m. gas and no m. ta activity can be noticed. Because of surface electrodes, here the m. gas EMG can also represent sol muscle activity in cases where it was selected by the optimization criteria. Neither m. vm or m. rf are active in the posture observed. The presence of EMG activity in the knee extensors supports the adequacy of m. smt activation in the computer optimization. Therefore, comparing this EMG to *Figure 6b* it could be stated that the measured EMG activity in the observed case is in good agreement with the muscles activated by the optimization criteria. This is also valid in other cases.

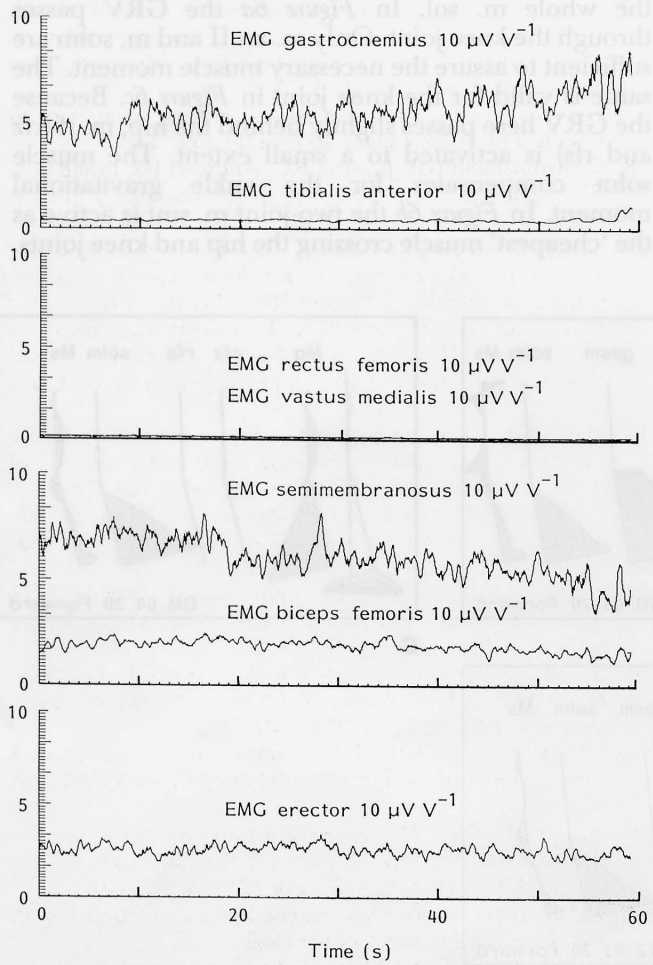

Figure 7 Integrated EMG record as measured for subject GB, measurement trial 03 in *forward-leaning posture*. Moments calculated with the model for this trial are shown in *Figure 6b*

In *Figures 5* and *6*, it can be noticed that the m. sol bending moment shape or the tibia bone stress profile appears as a triangle and the m. gas bending moment as a rectangular shape. For the femur, m. vl and m. vm have characteristic profiles as depicted in *Figures 5a, 5b, 5d* and *6d* arising from the long origins of these muscles. The m. smt (*Figure 6b*) profile is an irregular rectangular shape which appears to be characteristic also for the other two-joint muscles. The m. am profile will be discussed later.

From the entire procedure of calculating moments explained so far, it is evident and important that the muscle force calculation procedure did not include minimizing the bending moment M_S over the bone length as a criterion function. The only condition set was the satisfying of joint equilibrium equations (3), (4), (5) and the muscle force minimizing function (8), which includes satisfying the additional conditions (6). Nevertheless, just from *Figures 5* and *6* it is quite easy to see that a significant reduction of the resultant moment (M_S) over the whole bone was obtained. Therefore, it can be concluded and is important to notice that muscle forces produce such bending moments along the bone (M_M) that the resulting moment (M_S) is considerably decreased always, and for both the tibia and the femur, if compared to the gravitational moment (M_G). The resultant moments (M_S) are even better reduced in the case of the forward-leaning standing posture presented in *Figure 6*. As the GRV passes far from the bone's central line, the gravitational moment is substantially higher than in the voluntarily selected postures. In observing the resultant moments (M_S), it can be noticed that very high gravitational moments (M_G) are successfully compensated for by muscle moments. Larger resultant moment (M_S) values can be observed only on the top of the femur (*Figures 5a, b* and *6a, b*). This is the result of m. am (amI and amII) or m. smt activation. The z coordinates of the origin of these muscles are lower than the highest point of the femur. Therefore, the muscle lever for the pelvic bone is rather inaccurately determined. When observing the tibial bone, the moment M_S has the same sign in most of the cases recorded. This is a result of m. sol (soll, solm) and m. gas (gasl, gasm) activation.

In examining and comparing the M_S moments in *Figures 5* and *6*, it can be noticed that the profiles of bone-bending load moments have in all cases similar shapes and mirror the muscle action. The resulting moments have similar shapes in both body postures. These results confirm the expectation that orchestrated muscle force activation produces bending moment M_S of similar shapes in different body postures. Our results, therefore, grossly support and provide proof for the validation of the principle of minimal bone stress stated by Pauwels[3].

CONCLUSIONS

The work presented here, experimentally and grossly,

proves the principle of bending stress reduction of a long bone provoked by orchestrated muscle activity. It supports and additionally proves Pauwels' hypothesis[3,25] of the bending moment reduction by muscular activities. Pauwels also proposed that muscular action cannot be studied without considering the bone function and loading. Muscles not only provide the necessary moment equilibrium in all joints but also serve to compensate and reduce the bending stress while increasing the axial compressive load *regardless of posture*. Furthermore, the bone shape adapts to the external loading and muscle action[28] so as to minimize the bone stress. Therefore, the bone shape also reflects previous external loading and muscle action. Muscle function is very finely tuned to the functioning of bones, joints and ligaments. As a result, the bone as a load-carrying structure can be built with less material and can be lighter. Obviously, any column carrying less load can be built slimmer and thus with less material. Here it was observed that this is valid also for the musculo-skeletal system construction and functioning. It further means that nature uses active muscle force to ensure minimal bone stress and minimal bone weight and simultaneously to optimize efficient use of metabolic and muscular energy. It is quite probable that the human neurocontrol system, with its corresponding sensors, follows the criteria of bone bending minimization when synergistic muscle activation patterns are used in particular limb movements.

In comparing our findings to the results of Koch[2] and Pauwels[3] it can be concluded that the theoretical predictions of Pauwels are at least grossly proven by this work to be valid also for *in vivo* situations. Koch, in his work, did not include all the aspects and muscle moments actually acting across the bone. His work is mostly related to the properties and internal structure of the femoral bone while influence of muscle activity on stress in bone is not discussed in detail. Pauwel's work was more detailed, considering bending and also shearing moments. He considered both sagittal and coronal planes, explaining bending moment reduction by adding and also optimizing the activity of adequate muscles. Pauwels did not mathematically state the optimization procedure used for sharing the calculations among different muscles. In our model all muscles relevant for a forward–backward-leaning standing posture were included. Even though few assumptions are included in the model this study represents very detailed novel investigation of Pauwels' hypothesis. An important contribution, verified by the results presented, is the idea that the hypothesis is not only a mechanical principle describing musculo-skeletal system construction, but also the principle of selection of muscle, its level of activation and its force control. Furthermore, our findings are based on anatomical specimen data and on kinesiological measurements carried out on standing subjects. Because of large deviations in anthropometric data, accuracy of anatomical measurements and simplifications of data used in the computer model, the calculated results can be considered as gross results. Even from that point of view the results obtained strongly support the principles of Pauwels. Therefore, the results given can be considered as a pilot *in vivo* study for a gross evaluation of the stated principles, but future work is necessary for refinement of the presented approach.

ACKNOWLEDGEMENTS

This study was supported in part by Research Grant No. H133C80011 from the National Institute on Disability and Rehabilitation Research, Washington DC, and the Slovene Research Council, Ljubljana, Slovenia.

We would like to thank, for all suggestions, Prof. Dr A. Sirca, Prof. Dr A Dekleva, L. Travnik, MD and Milan Stevanec, Res. Assoc., from Anatomical Institute of Medical Faculty, Ljubljana, Slovenia.

REFERENCES

1. Baron JB. History of posturography. *7th Int Soc Posturography*, Houston, TX 1983, 54–9.
2. Koch, JC. The laws of bone architecture. *Am J Anat* 1917; **21:** 177–293.
3. Pauwels F. *Biomechanics of the Locomotor Apparatus*. Berlin: Springer-Verlag, 1980.
4. Chow CK, Jacobson DH. Studies of human locomotion via optimal programming. *Math Biosc* 1971; **10:** 239–306.
5. Hatze H. A comprehensive model for human motion simulation and its application of the take-off phase of the long jump. *J Biomech* 1981; **14:** 135–42.
6. Hoy MG, Zajac FE, Gordon ME. A musculoskeletal model of the human lower extremity: the effect of muscle, tendon and moment arm on the moment-angle relationship of musculotendon actuators at the hip, knee, and ankle. *J Biomech* 1990; **23:** 157–69.
7. Hill AV. The abrupt transition from rest to activity in muscle *Proc R Soc London* 1949; **136:** 399.
8. Crowninshield RD, Jonston RC, Andrews JG, Brand RA, Biomechanical investigation of the human hip. *J Biomech* 1978; **11** 75–85.
9. Dul J, Townsend MA, Shiavi R, Johnson GE. Muscular synergism – I: on criteria for load sharing between synergistic muscles. *J Biomech* 1984; **17:** 663–74.
10. Dul J, Johnson GE, Shiavi R, Townsend MA. Muscular synergism – II: a minimum-fatigue criterion for load sharing between synergistic muscles. *J Biomech* 1984; **17:** 675–84.
11. Hardt DE. Determining muscle forces in the leg during normal human walking – an application and evaluation of optimization methods. *J Biomech Eng* 1978; **100:** 72–8.
12. Seireg A, Arkivar RJ. A mathematical model for evaluation of forces in lower extremities of the musculo-skeletal system. *J Biomech* 1973; **6:** 313–26.
13. Seireg A, Arkivar RJ. The prediction of muscular load sharing and joint forces in the lower extremities during walking. *J Biomech* 1975; **8:** 89–102.
14. Brand RA, Crowninshield RD, Wittstock CE, Pederson DR, Clark CR. A model of lower extremity muscular anatomy. *J Biomech Eng* 1982; **104:** 304–10.
15. Dostal WF, Andrews JG. A three-dimensional biomechanic model of the hip musculature. *J Biomech* 1981; **14:** 803–12.
16. Jensen RH, Davy DT. An investigation of muscle lines of action about the hip: A centroid line approach vs the straight line approach. *J Biomech* 1975; **8:** 103–10.
17. Fick R. *Handbuch der Anatomie und Mechanik der Gelenke I, II, IIB*. Jena: Verlag von Gustav Fischer, 1911.
18. Maquet PGJ. *Biomechanics of the Knee*. Berlin: Springer-Verlag, 1984.
19. Winter DA Biomechancis of human movement with applications to the study of human locomotion. *CRC*

Critical Reviews in Biomed Eng 1979; **9:** 287–314.
20. Kralj A, Bajd T. *Functional Electrical Stimulation: Standing and Walking After Spinal Cord Injury*. Boca Raton, FL: CRC Press, 1989.
21. Mansour JM, Adu ML. The passive elastic moment of the knee and its influence on human gait. *J Biomech* 1986; **29:** 369–73.
22. Yoon YS, Mansour JM. The passive elastic moment at the hip. *J Biomech* 1982; **15:** 905–10.
23. Pedotti A, Krishnan VV, Stark L. Optimization of muscle force sequencing in human locomotion. *Math Bioci* 1978; **38:** 57–76.
24. Kralj A. Optimum coordination and selection of muscles for functional electronic stimulation. *Proc 8th ICMBE*, Chicago, 1969.
25. Munih M, Kralj A, Badj T, Jaeger R. Bone bending profiles in standing. *12th Annual Conf RESNS*, New Orleans, 1989, 667–767.
26. Martens M, Van Audekercke R, De Meester P, Mulier JC. The mechanical characteristics of the long bones of the lower extremity in torsional loading. *J Biomech* 1980; **13:** 667–767.
27. Beaupre GS, Vasu R, Carter DR, Schurman DJ. Epiphyseal-based designs for tibial plateau components – II: stress analysis in the sagittal plane. *J Biomech* 1986; **19:** 663–73.
28. Lovejoy CO. Evolution of human walking. *Scientific American* 1988; **259:** 82–9.